

2-16-2017

Formation of environmentally persistent free radicals (EPFRs) on ZnO at room temperature: Implications for the fundamental model of EPFR generation.

Matthew C. Patterson
Louisiana State University, Baton Rouge

Mark F. DiTusa
Louisiana State University, Baton Rouge

Cheri A. McFerrin
Department of Natural Sciences and Mathematics, Dominican University of California

R. L. Kurtz
Louisiana State University, Baton Rouge

Randall W. Hall
Department of Natural Sciences and Mathematics, Dominican University of California,
randall.hall@dominican.edu

Survey: Let us know how this paper benefits you.

See next page for additional authors

<https://doi.org/10.1016/j.cplett.2016.12.061>

Recommended Citation

Patterson, Matthew C.; DiTusa, Mark F.; McFerrin, Cheri A.; Kurtz, R. L.; Hall, Randall W.; Poliakoff, E. D.; and Sprunger, P. T., "Formation of environmentally persistent free radicals (EPFRs) on ZnO at room temperature: Implications for the fundamental model of EPFR generation." (2017). *Natural Sciences and Mathematics | Faculty Scholarship*. 29.
<https://doi.org/10.1016/j.cplett.2016.12.061>

This Article is brought to you for free and open access by the Department of Natural Sciences and Mathematics at Dominican Scholar. It has been accepted for inclusion in Natural Sciences and Mathematics | Faculty Scholarship by an authorized administrator of Dominican Scholar. For more information, please contact michael.pujals@dominican.edu.

Authors

Matthew C. Patterson, Mark F. DiTusa, Cheri A. McFerrin, R. L. Kurtz, Randall W. Hall, E. D. Poliakoff, and P. T. Sprunger



HHS Public Access

Author manuscript

Chem Phys Lett. Author manuscript; available in PMC 2018 February 16.

Published in final edited form as:

Chem Phys Lett. 2017 February 16; 670: 5–10. doi:10.1016/j.cplett.2016.12.061.

Formation of environmentally persistent free radicals (EPFRs) on ZnO at room temperature: Implications for the fundamental model of EPFR generation

Matthew C. Patterson^{1,*}, Mark F. DiTusa², Cheri A. McFerrin³, R.L. Kurtz², Randall W. Hall³, E. D. Poliakoff¹, and P. T. Sprunger²

¹Department of Chemistry, Louisiana State University, Baton Rouge, LA 70803, USA

²Department of Physics and Astronomy, Louisiana State University, Baton Rouge, LA 70803, USA

³Department of Natural Sciences and Mathematics, Dominican University of California, San Rafael, CA 94901, USA

Abstract

Environmentally persistent free radicals (EPFRs) have significant environmental and public health impacts. In this study, we demonstrate that EPFRs formed on ZnO nanoparticles provide two significant surprises. First, EPR spectroscopy shows that phenoxy radicals form readily on ZnO nanoparticles at room temperature, yielding EPR signals similar to those previously measured after 250°C exposures. Vibrational spectroscopy supports the conclusion that phenoxy-derived species chemisorb to ZnO nanoparticles under both exposure temperatures. Second, DFT calculations indicate that electrons are transferred from ZnO to the adsorbed organic (oxidizing the Zn), the opposite direction proposed by previous descriptions of EPFR formation on metal oxides.

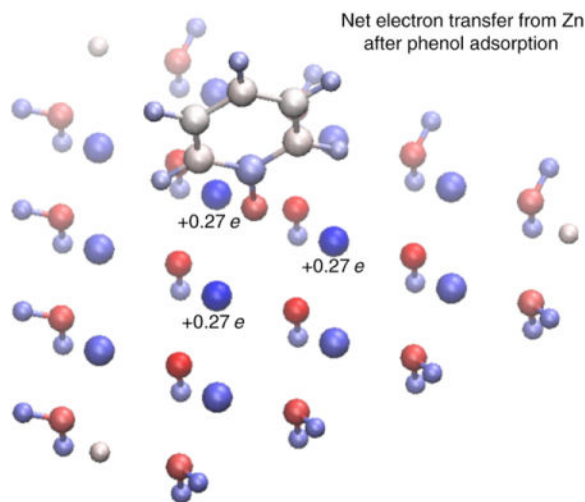
Graphical abstract

*Corresponding Author; mpatt15@lsu.edu.

Publisher's Disclaimer: This is a PDF file of an unedited manuscript that has been accepted for publication. As a service to our customers we are providing this early version of the manuscript. The manuscript will undergo copyediting, typesetting, and review of the resulting proof before it is published in its final citable form. Please note that during the production process errors may be discovered which could affect the content, and all legal disclaimers that apply to the journal pertain.

Supporting Information

Details of experimental and computational methods.



Introduction

The impact of particulate matter (PM) on human health has become a major environmental issue recognized by government agencies¹⁻³. The toxicity of transition metal-containing PM is significantly increased by the formation of environmentally persistent free radicals (EPFRs) – composite metal oxide/organic radical complexes with lifetimes of hours or days under ambient conditions^{3,4}. EPFR-containing PM has been demonstrated to produce pulmonary and cardiovascular dysfunction in animal models, with greater toxicity than non-EPFR-containing PM⁵⁻¹¹. EPFRs were first proposed to form through the reduction of metal oxides by high-temperature exposure (above 150°C) to simple substituted aromatics, which electron and X-ray spectroscopy has shown to occur on CuO^{12,13} and TiO₂¹⁴ model systems. However, the longest-lived EPFR species observed to date are phenoxy radicals generated on ZnO¹⁵, which presents a significant challenge to the generic model of EPFR formation because it is usually not possible to create a Zn(I) oxidation state except under rare conditions¹⁶⁻²⁰. The extraordinary longevity of ZnO-generated EPFRs – lifetimes of 73 days in ambient conditions – suggests that Zn-containing PM may present an ongoing environmental hazard throughout remediation processes.

A previous single crystal photoelectron spectroscopy study of phenol adsorption on ZnO²¹ hinted at two surprising results. First, band bending suggested that electron density was transferred from the ZnO to the adsorbate, i.e., the opposite direction of what has been proposed for EPFR formation. Second, the same band bending was observed after RT and high temperature exposure, suggesting that the adsorption occurs readily at room temperature. This study attempts to clarify those earlier results. Here we work on ZnO nanoparticles, which are more realistic PM surrogates. This enables us to obtain EPR data demonstrating the formation of EPFRs, which is not feasible on single-crystal samples. We also present vibrational spectroscopy that corroborates and complements the preliminary photoelectron results. Finally, we show theoretical calculations supporting the proposed direction of charge transfer and suggesting that the favorable binding site for the phenoxy/ZnO EPFR involves coordination to three Zn cations, a departure from previous

models involving the reduction of a single cation by the organic. A schematic of these two opposing mechanisms is depicted in Figure 1. The current results elucidate fundamental details of the formation of phenol-derived EPFR species over ZnO nanoparticles, verifying that these EPFRs on ZnO form at RT. We discuss these anomalous results in terms of their implications for the generic picture of EPFR formation and the stability and longevity of ZnO-derived EPFRs.

Methods

Sample preparation

ZnO powder with average diameter 18nm ($\sim 60 \text{ m}^2/\text{g}$) was purchased from US Research Nanomaterials. Phenol (CAS 108-95-2, ACS reagent grade, 99.0% pure) was purchased from Sigma-Aldrich and degassed by freeze-pump-thaw cycles before exposing samples.

Samples were prepared using a custom-built vacuum dosing manifold similar to that used in prior EPR experiments²²; the main difference between our apparatus and that used for prior work is that our dosing chamber is made of stainless steel and pumped by a turbomolecular pump with base pressure below 10^{-4} mbar. “Blank” (un-dosed) samples for all measurements were prepared by heating the samples to 250°C for 1 hour while being pumped by the turbo, then cooling to RT while pumping. For elevated temperature exposures, samples were brought to a stable temperature of 250°C while being pumped by the turbo.

For EPR and FTIR measurements, samples were dosed by closing the valve to the pump and opening the valves to the phenol and sample tubes, allowing phenol vapor to equilibrate throughout the system (at RT, a vapor pressure of ~ 0.4 mbar) for 1 hour with the sample at the desired dosing temperature. After exposure, the phenol valve was closed and the sample tube pumped back down to the base pressure of the turbo (while cooling to RT if necessary).

For INS measurements, approximately 0.01 mol (0.94 g) of phenol was loaded into the bottom of a steel sample tube, then 4 g ZnO powder was packed on top of the phenol to fill the tube. (This ensured that enough ZnO mass was present to give a strong signal from the relatively weak neutron scattering process.) The tube was attached to the dosing system and pumped out to the turbo base pressure, then closed and heated to 250°C for 1 hour. This ensured that phenol vapor diffused throughout and reacted with the entire sample. After exposure, the sample tube was evacuated while cooling to RT before removal from the dosing system for measurement.

Samples were analyzed under ambient conditions at RT using EPR spectroscopy and FTIR spectroscopy, and under high vacuum at 5K using INS at the VISION beamline²³ at the Spallation Neutron Source at Oak Ridge National Laboratory.

Density functional calculations were performed using the NWChem program²⁴ and natural bond order analysis was performed using the NBO program²⁵. Full details on experimental apparatus and the measurement and computational procedures are given in the supporting information.

Results

EPR spectroscopy reveals the presence and nature of an unpaired electron species after exposure of ZnO nanoparticles to phenol at RT. The g -factor of 2.0044 and H_{p-p} value of 5.4 G are broadly consistent with previously measured values for silica-supported ZnO nanoparticles exposed to phenol at 230°C¹⁵. The narrow signal suggests only one radical species present after RT chemisorption. Computational modeling coupled with vibrational studies help us unravel the atomistic details of the radicals detected by EPR.

DFT modeling of adsorbates on a $Zn_{12}O_{19}C_6H_{38}$ cluster suggests one possible binding configuration for a phenoxy species, depicted in Figure 3. (The cluster modeled here may be thought of as representative of a Zn(0001)-Zn terminated surface; H atoms terminate the model cluster to maintain formal charge neutrality, and the overall cluster is neutral with a singlet spin state with $S^2=0$.) The phenoxy chemisorbs through its oxygen atom and coordinates to three Zn atoms. Table 1 gives the calculated charges on each Zn atom in the model cluster with and without the attached phenoxy species. Most of the Zn atoms become slightly less positive after adsorption by a negligible magnitude of 0.027 e or less. (Charges on the cluster O atoms change by similarly negligible amounts.) The overall charge of the phenoxy moiety given by NBO analysis is $-0.86e$, and the overall charge on the metal oxide moiety is $+0.86e$. Three Zn atoms coordinate to the adsorbed phenoxy (atoms 5, 8, and 9 in Figure 3 and Table 1) with an average distance of 2.30 Å. Comparing this distance to the known Zn-O distance in solid ZnO of 1.98 Å²⁶ and the calculated Zn-O distance in a gas phase Zn-O dimer of 1.72 Å²⁷ indicates partial bonding of the phenoxy oxygen atom to each of the three closest Zn atoms. Each of the three Zn atoms becomes more positive after adsorption by just over 0.27 e . That is, the Zn atoms coordinated to the phenoxy are *oxidized*, not *reduced*, upon adsorption. It is significant that even though $-0.86e$ is collectively transferred to the adsorbed organic, no single Zn atom loses an entire electron's worth of negative charge – in other words, this calculation does not suggest that a lone-oxidized Zn(III) species is created. The calculated transfer of electrons from the ZnO toward the adsorbed phenoxy is, again, consistent with prior photoelectron studies of phenol adsorption on ZnO single crystals.

Figure 4 depicts FT-IR spectra in the fingerprint region, 900–1800 cm^{-1} , for phenol adsorbed on ZnO nanoparticles at RT and 250°C, as well as a reference spectrum of solid phenol. Peaks corresponding to the phenol reference spectrum are present after adsorption at both temperature conditions, implying the presence of a phenol or phenoxy-like surface species. (The major exception is the broad feature in the adsorbed spectra between 1340–1460 cm^{-1} , which we attribute to an incompletely subtracted bulk ZnO feature.) We observe two key features of chemisorption after exposure to ZnO nanoparticles at both temperatures – the two peaks at 1471 and 1497 cm^{-1} from solid phenol (black) collapse to a single peak at 1491 cm^{-1} in both of the exposed spectra (red and blue), and the broad band peaked at 1224 cm^{-1} in solid phenol blueshifts to three distinct peaks at 1246, 1267, and 1279 cm^{-1} in the adsorbed spectra. The former peaks at 1474 and 1497 cm^{-1} are attributed to combinations of $\nu(CC) + \nu(CO)$ and $\delta(CH) + \nu(CC)$ modes respectively in solid phenol, and the broad band peaked at 1224 cm^{-1} is a manifold of $\delta(OH)$ and $\nu(CO)$ modes. The constraint of the ring-breathing and C–H bending modes to one peak at 1491 cm^{-1} is consistent with a

chemisorbed surface species, as is the loss of the broad manifold of hydrogen-bonded O–H bending modes around 1224 cm^{-1} – this is indicative of a dissociative adsorption mechanism to the ZnO surface resulting in a chemisorbed phenoxy-type surface species. In Figure S1 of the Supporting Information, we show the calculated infrared absorption spectrum from the cluster model shown in Figure 2, which agrees reasonably well with the experimental data.

It is immediately apparent that the only significant differences in the FTIR spectra between phenol adsorbed at RT and phenol adsorbed at 250°C are slight differences in peak intensity ratios (see e.g. the three peaks between $1240 - 1280\text{ cm}^{-1}$). No peak shifts are noted, which strongly implies that the same chemisorbed species is present under both temperature conditions.

Additional characteristic vibrational modes of the ZnO EPFR system are depicted in Figure 5, which presents a comparison between FTIR and INS spectra over the same energy region (Figure 5a) for phenol exposure at 250°C , as well as a region inaccessible to benchtop FTIR (Figure 5b). Figure 5a shows the C–H “oop” bending modes of phenol, the most intense of which appear at 687 and 749 cm^{-1} for solid phenol in FTIR (Figure 5a, upper pane, black spectrum). These modes are both blueshifted after phenol chemisorption at 250°C , by 6.1 and 14.3 cm^{-1} respectively. The equivalent INS data shows similar shifts after high temperature adsorption (Figure 5a, lower pane).

INS can interrogate vibrational peaks at substantially lower frequencies than a lab IR spectrometer, and additionally is sensitive to dipole-inactive vibrational modes. Figure 5b presents one such peak at 410 cm^{-1} (pure solid phenol, black spectrum). The corresponding mode is an out-of-plane twist of the phenyl ring, involving a large displacement of hydrogen atoms but almost zero change in dipole moment, which is ideal for INS but not FTIR. We see also a blueshift in this mode of approximately 5.1 cm^{-1} .

Discussion

Taken together, the FTIR and INS results suggest that there are only minor differences in the surface species present after ZnO nanoparticles are exposed to phenol at RT and 250°C , and all the spectra are consistent with chemisorption of a phenoxy species (that is, a deprotonated phenol molecule with a reasonably strong bond to the surface) at both temperatures. This is consistent with our prior ultraviolet photoelectron spectroscopy results²¹, which showed that the valence band electronic structure (including the occupied molecular orbitals of the organic adsorbate) of phenol-exposed ZnO surfaces was nearly identical after RT and high temperature adsorption.

The present data are straightforward to interpret. EPR suggests that after ZnO nanoparticles are exposed to phenol vapor at RT, a radical species is present with a g -factor characteristic of a phenoxy-type radical. Vibrational spectroscopy suggests that at both RT and 250°C , phenol chemisorbs to these ZnO nanoparticles and forms a surface-bound phenoxy species, and DFT calculations provide a model structure for the chemisorbed species and suggest that $-0.86e$ is transferred to the organic from the coordinated surface Zn atoms. All of these results are consistent with previous studies of phenol adsorption on ZnO single crystals or

ZnO nanoparticles exposed to phenol at elevated temperature^{15,21}. The existence of an EPFR after chemisorption at RT corroborates the extraordinarily long half-life of ZnO-derived EPFRs under ambient conditions, as it suggests that the equilibrium between EPFRs and their decay products should thermodynamically favor the EPFR side.

However, this interpretation of the present data contradicts both the conventional model of EPFR formation and the common-sense picture of the redox activity of Zn. No Zn(III) compounds are known in nature, and even theoretical predictions of their existence are contested^{28,29}, so in no way do we mean to suggest here that phenol oxidizes Zn(II) to Zn(III). And while Zn(I) compounds have been synthesized, they are “commonly” seen as $[\text{Zn}_2]^{2+}$ dimers^{17,19,20} or isolated Zn^+ cations immobilized in bulky zeolite matrices^{16,18}. It should be almost as implausible to say that either a Zn(I) or Zn(III) species accompanies EPFR formation on ZnO.

This presents a challenge to our general model of EPFR formation, because ZnO cannot fit into the redox paradigm established for other metal oxides such as CuO. This suggests that a more generalizable model is necessary to capture an accurate description of EPFR formation. We suggest instead viewing this process as a classic problem of band/molecular orbital alignment in a semiconductor. In this picture, we would say that if molecular energy levels and the band structure of the metal oxide align correctly, the LUMO of an organic molecule may hybridize with occupied electronic states in the semiconductor, leading to a net electron transfer toward the molecule and a shift in energy of the semiconductor valence bands toward the Fermi level (“upward band bending”) after chemisorption³⁰. On the other hand, in a different material it may be more favorable for the HOMO of an adsorbate to hybridize with unoccupied states in the surface, leading to electron transfer out of the HOMO and a band bending downward (away from the Fermi level).

In this paradigm, the parameters of importance are the electronic properties of the metal oxide and organic – the alignment of molecular energy levels with occupied and unoccupied bands in the oxide. These electronic properties are accessible by both experiment and calculation, and reference to the well-developed band theory of semiconductors may prove fruitful in the interpretation of EPFR properties such as lifetime, photochemical activity, and decay modes. Moreover, such a model better captures the details of previous work regarding phenol adsorption and charge transfer in ZnO and TiO_2 single crystals, as these two systems provide excellent examples of “upward” and “downward” band bending respectively after chemisorption (in addition to more explicit signatures of electron transfer)^{14,21,31}.

To summarize briefly, we have shown that room temperature phenol adsorption on ZnO nanoparticles produces a phenoxy-type radical similar to previously characterized EPFR species produced on supported ZnO at higher temperature exposures. FTIR and INS measurements verify the presence of nearly identical chemisorbed phenoxy species after both RT and 250°C exposure. DFT calculations suggest that adsorption oxidizes the Zn atoms coordinated to the phenoxy, which disrupts the “conventional” redox picture of EPFR formation due to the improbability of creating a Zn(III) species. We suggest that this conventional picture is only an incomplete description of the model of EPFR formation, and

that an analysis of EPFR formation from the perspective of semiconductor band theory may prove a more fruitful approach.

Supplementary Material

Refer to Web version on PubMed Central for supplementary material.

Acknowledgments

The authors acknowledge support from the National Institute of Environmental Health Sciences Superfund Research Program through Grant P42 ES013648-03. The INS material is based upon work supported by the U.S. Department of Energy under EPSCoR Grant No. DE-SC0012432 with additional support from the Louisiana Board of Regents; moreover, this research benefited from the use of the VISION beamline at ORNL's Spallation Neutron Source, which is supported by the Scientific User Facilities Division, Office of Basic Energy Sciences, U.S. Department of Energy under Contract No. DE-AC0500OR22725. Calculations were performed using the High Performance Computing resources at Louisiana State University. RWH acknowledges support from Dominican University of California's Lillian L.Y. Wang Yin, PhD Endowment. The authors thank Luke Daemen and Yongqiang Cheng of ORNL for their invaluable assistance with INS measurements at VISION, as well as Kresimir Rupnik for consultation regarding EPR spectroscopy.

References

1. Kloog I, Nordio F, Zanobetti A, Coull BA, Koutrakis P, Schwartz JD. Short Term Effects of Particle Exposure on Hospital Admissions in the Mid-Atlantic States: a Population Estimate. *PLoS ONE*. 2014; 9(2):e88578. [PubMed: 24516670]
2. Guarnieri M, Balmes JR. Outdoor Air Pollution and Asthma. *The Lancet*. 2014; 383(9928):1581–1592.
3. Dugas TR, Lomnicki S, Cormier SA, Dellinger B. Addressing Emerging Risks: Scientific and Regulatory Challenges Associated with Environmentally Persistent Free Radicals. *International Journal of Environmental Research and Public Health*. 2016; 13(6):573.
4. Cruz dela ALN, Cook RL, Dellinger B, Lomnicki SM, Donnelly KC, Kelley MA, Cosgriff D. Assessment of Environmentally Persistent Free Radicals in Soils and Sediments From Three Superfund Sites. *Environ Sci: Processes Impacts*. 2014; 16(1):44–52.
5. Lee GI, Saravia J, You D, Shrestha B, Jaligama S, Hebert VY, Dugas TR, Cormier SA. Exposure to Combustion Generated Environmentally Persistent Free Radicals Enhances Severity of Influenza Virus Infection. *Part Fibre Toxicol*. 2014; 11(1):57. [PubMed: 25358535]
6. Balakrishna S, Saravia J, Thevenot P, Ahlert T, Lominiki S, Dellinger B, Cormier SA. Environmentally Persistent Free Radicals Induce Airway Hyperresponsiveness in Neonatal Rat Lungs. *Part Fibre Toxicol*. 2011; 8(1):11. [PubMed: 21388553]
7. Reed JR, Cruz dela ALN, Lomnicki SM, Backes WL. Environmentally Persistent Free Radical-Containing Particulate Matter Competitively Inhibits Metabolism by Cytochrome P450 1A2. *Toxicol Appl Pharmacol*. 2015; 289(2):223–230. [PubMed: 26423927]
8. Reed JR, Cruz dela A, Lomnicki SM. Inhibition of Cytochrome P450 2B4 by Environmentally Persistent Free Radical-Containing Particulate Matter. *Biochemical ...*. 2015
9. Balakrishna S, Lomnicki S, McAvey KM, Cole RB, Dellinger B, Cormier SA. Environmentally Persistent Free Radicals Amplify Ultrafine Particle Mediated Cellular Oxidative Stress and Cytotoxicity. *Part Fibre Toxicol*. 2009; 6(1):11. [PubMed: 19374750]
10. Lord K, Moll D, Lindsey JK, Mahne S, Raman G, Dugas T, Cormier S, Troxclair D, Lomnicki S, Dellinger B, et al. Environmentally Persistent Free Radicals Decrease Cardiac Function Before and After Ischemia/Reperfusion Injury in Vivo. *Journal of Receptors and Signal Transduction*. 2011; 31(2):157–167. [PubMed: 21385100]
11. Burn BR, Varner KJ. Environmentally Persistent Free Radicals Compromise Left Ventricular Function During Ischemia/Reperfusion Injury. *Am J Physiol Heart Circ Physiol*. 2015; 308(9):H998–H1006. [PubMed: 25681431]

12. Alderman SL, Farquar GR, Poliakoff ED, Dellinger B. An Infrared and X-Ray Spectroscopic Study of the Reactions of 2-Chlorophenol, 1,2-Dichlorobenzene, and Chlorobenzene with Model CuO/Silica Fly Ash Surfaces. *Environ Sci Technol.* 2005; 39(19):7396–7401. [PubMed: 16245807]
13. Farquar GR, Alderman S, Poliakoff E, Dellinger B. X-Ray Spectroscopic Studies of the High Temperature Reduction of Cu(II)O by 2-Chlorophenol on a Simulated Fly Ash Surface. *Environ Sci Technol.* 2003; 37(5):931–935. [PubMed: 12666923]
14. Patterson MC, Thibodeaux CA, Kizilkaya O, Kurtz RL, Poliakoff ED, Sprunger PT. Electronic Signatures of a Model Pollutant-Particle System: Chemisorbed Phenol on TiO₂(110). *Langmuir.* 2015; 31(13):3869–3875. [PubMed: 25774565]
15. Vejerano E, Lomnicki S, Dellinger B. Lifetime of Combustion-Generated Environmentally Persistent Free Radicals on Zn(I)O and Other Transition Metal Oxides. *J Environ Monit.* 2012; 14(10):2803. [PubMed: 22990982]
16. Tian Y, Li G-D, Chen J-S. Chemical Formation of Mononuclear Univalent Zinc in a Microporous Crystalline Silicoaluminophosphate. *J Am Chem Soc.* 2003; 125(22):6622–6623. [PubMed: 12769558]
17. Wang X, Andrews L. Infrared Spectra of Zn and Cd Hydride Molecules and Solids. *J Phys Chem A.* 2004; 108(50):11006–11013.
18. Zhen S, Bae D, Seff K. Zn⁺-Cations, Probable Tl₄Zn₁₂ and Tl₆Clusters, and Zeolite Desilication (Less Likely Dealumination): Crystallographic Study of the Incomplete Reaction of Zn Vapor with Tl⁺-Exchanged Zeolite X. *J Phys Chem B.* 2000; 104(3):515–525.
19. Gurrane A, Resa I, Rodriguez A, Carmona E, Alvarez E, Gutierrez-Puebla E, Monge A, Galindo A, del Río D, Andersen RA. Zinc–Zinc Bonded Zincocene Structures. Synthesis and Characterization of Zn₂(H₅-C₅Me₅)₂ and Zn₂(H₅-C₅Me₄Et)₂. *J Am Chem Soc.* 2007; 129(3):693–703. [PubMed: 17227033]
20. Resa I, Carmona E, Gutierrez-Puebla E, Monge A. Decamethylzincocene, a Stable Compound of Zn(I) with a Zn–Zn Bond. *Science.* 2004; 305(5687):1136–1138. [PubMed: 15326350]
21. Thibodeaux CA, Poliakoff ED, Kizilkaya O, Patterson MC, DiTusa MF, Kurtz RL, Sprunger PT. Probing Environmentally Significant Surface Radicals: Crystallographic and Temperature Dependent Adsorption of Phenol on ZnO. *Chemical Physics.* 2015; 638:56–60.
22. Lomnicki S, Truong H, Vejerano E, Dellinger B. Copper Oxide-Based Model of Persistent Free Radical Formation on Combustion-Derived Particulate Matter. *Environ Sci Technol.* 2008; 42(13):4982–4988. [PubMed: 18678037]
23. Seeger PA, Daemen LL, Larese JZ. Resolution of VISION, a Crystal-Analyzer Spectrometer. *Nuclear Instruments and Methods in Physics Research Section A: Accelerators, Spectrometers, Detectors and Associated Equipment.* 2009; 604(3):719–728.
24. Valiev M, Bylaska EJ, Govind N, Kowalski K, Straatsma TP, Van Dam HJJ, Wang D, Nieplocha J, Apra E, Windus TL, et al. NWChem: a Comprehensive and Scalable Open-Source Solution for Large Scale Molecular Simulations. *Computer Physics Communications.* 2010; 181(9):1477–1489.
25. Glendenning, ED., Badenhop, JK., Reed, AE., Carpenter, JE., Bohmann, JA., Morales, CM., Landis, CR., Weinhold, F. Nbo 6.0. Theoretical Chemistry Institute, University of Wisconsin; Madison: 2013.
26. Kihara K, Donnay G. Anharmonic Thermal Vibrations in ZnO. *Canadian Mineralogist.* 1985; 23:647–654.
27. NIST Computational Chemistry Comparison and Benchmark Database. Oct 18.2016
28. Schlöder T, Kaupp M, Riedel S. Can Zinc Really Exist in Its Oxidation State +III? *J Am Chem Soc.* 2012; 134(29):11977–11979. [PubMed: 22775535]
29. Samanta D, Jena P. Zn in the + III Oxidation State. *J Am Chem Soc.* 2012
30. Zhang Z, Yates JT. Band Bending in Semiconductors: Chemical and Physical Consequences at Surfaces and Interfaces. *Chem Rev.* 2012; 112(10):5520–5551. [PubMed: 22783915]
31. Patterson MC, Keilbart ND, Kiruri LW, Thibodeaux CA, Lomnicki S, Kurtz RL, Poliakoff ED, Dellinger B, Sprunger PT. EPFR Formation From Phenol Adsorption on Al₂O₃ And TiO₂: EPR and EELS Studies. *Chemical Physics.* 2013; 422:277–282. [PubMed: 24443627]

Highlights

- EPR spectroscopy indicates the formation of an aromatic radical after chemisorption of phenol on ZnO nanoparticles at room temperature
- Vibrational spectroscopy (FTIR and neutron scattering) indicates that the organic is a phenoxyl species, and identical to the previously identified phenoxyl radical species formed after exposure at 250°C
- DFT calculations indicate the phenoxyl radical is formed through electron transfer from the surface Zn atoms to the organic, oxidizing the Zn
- Due to the improbability of creating either a Zn(III) or a Zn(I) species, as well as the lack of thermal activation of the radical-forming reaction, these results suggest the conventional redox picture of environmentally persistent free radical formation on metal oxides is at best incomplete

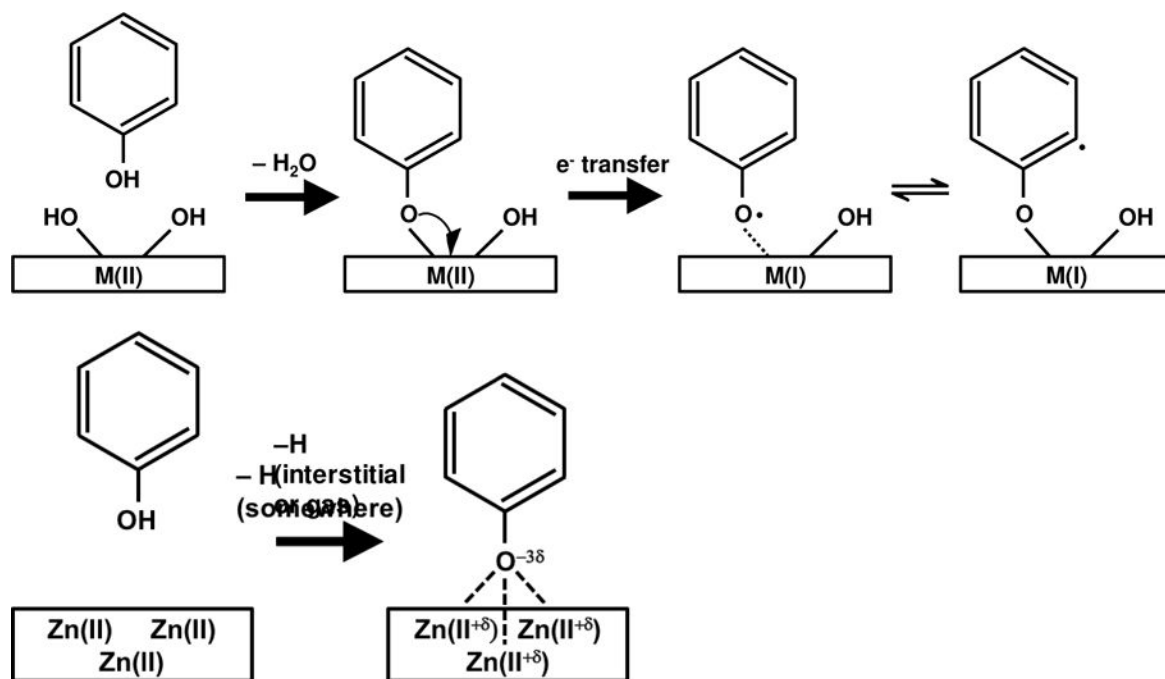


Figure 1.
 (top row) Schematic of EPFR formation from phenol adsorbed on a generic metal oxide.
 (bottom row) Schematic of EPFR formation from phenol adsorbed on ZnO; the proposed fate of the hydrogen atom is conjecture.

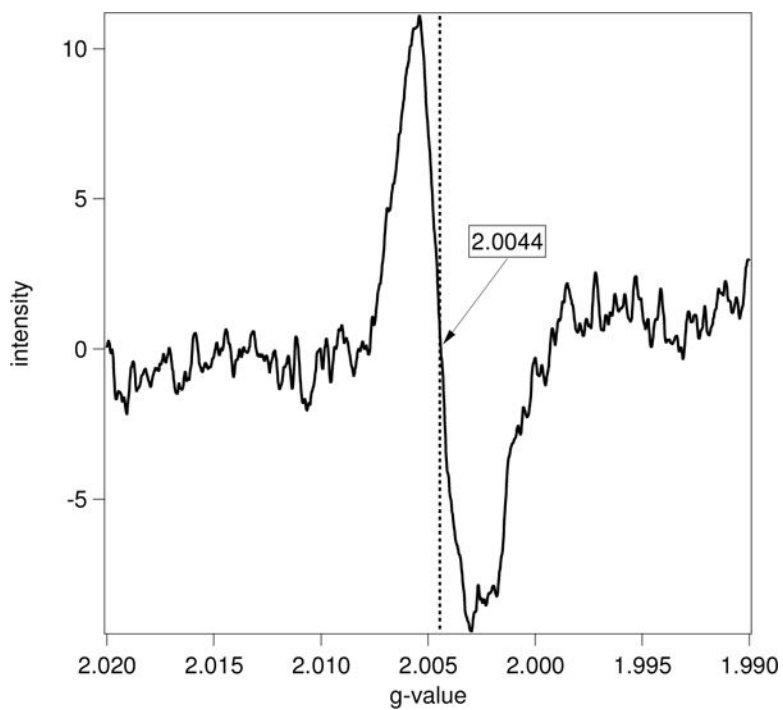


Figure 2.
EPR spectrum from ZnO nanoparticles exposed to phenol at RT.

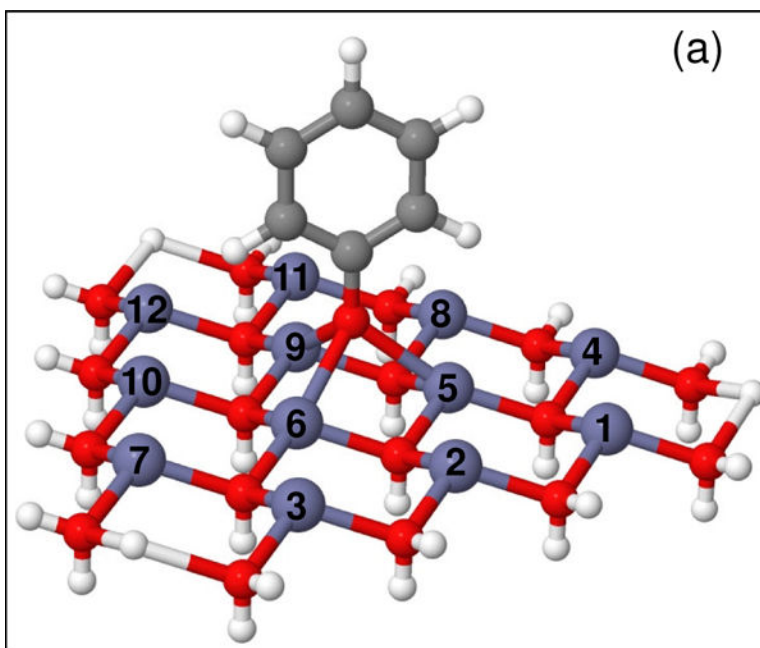


Figure 3.
(a) The $Zn_{12}O_{19}C_6H_{38}$ cluster used for our DFT calculations, illustrating the bonding geometry of the phenoxy species. C atoms are gray, H atoms are white, Zn atoms are blue, and O atoms are red. Zn atoms are numbered for convenience of display in Table 1.

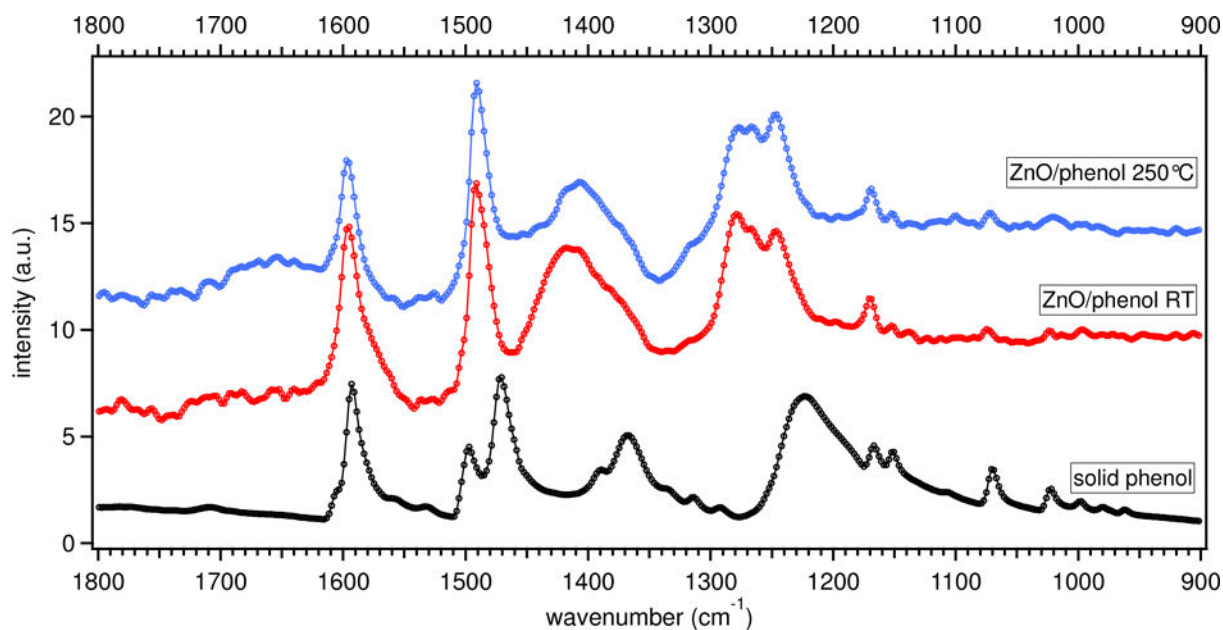


Figure 4. ATR-FTIR spectra of ZnO dosed with phenol at 250°C (top, blue) ZnO dosed with phenol at RT (middle, red), and solid phenol (bottom, black). A blank (un-dosed) ZnO spectrum has been subtracted from each of the dosed ZnO spectra.

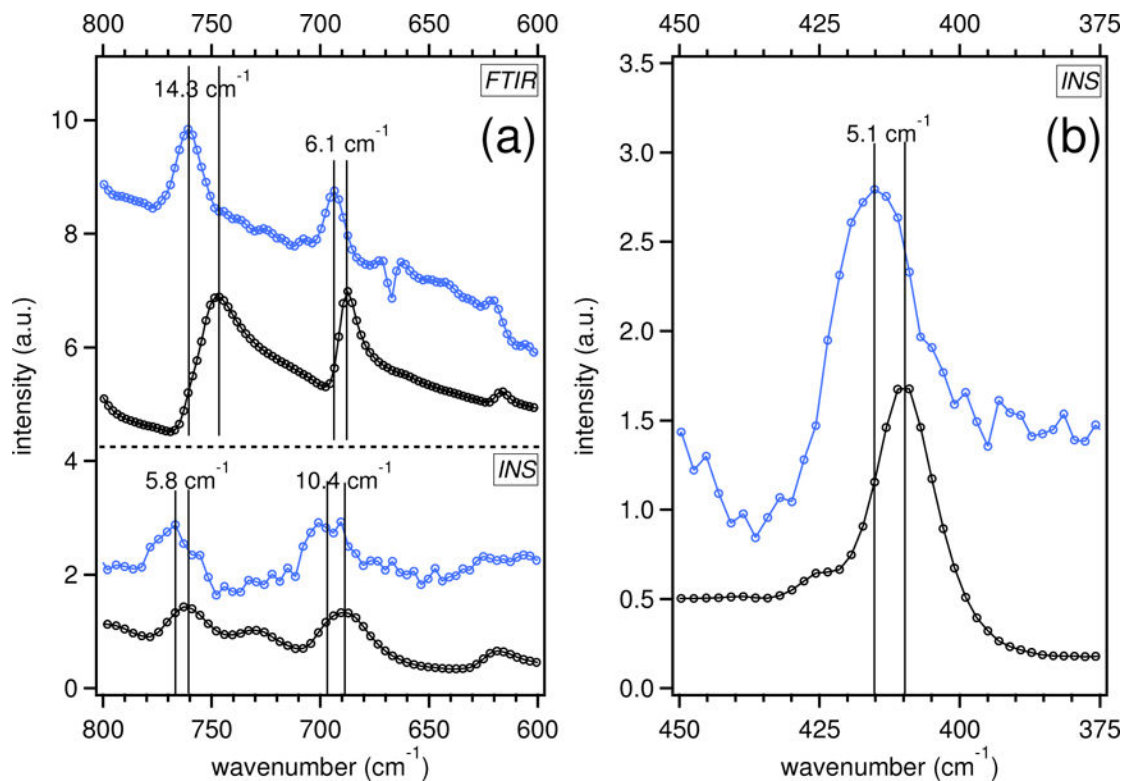


Figure 5.

Comparison of FTIR and INS spectra. Spectra in blue are from ZnO nanoparticles dosed with phenol at 250°C, spectra in black are from solid phenol. A blank (un-dosed) ZnO spectrum has been subtracted from each of the dosed ZnO spectra. All INS spectra are displayed with background corrections for the sample containers; additionally a blank (un-dosed) ZnO spectrum has been subtracted from the ZnO INS spectra to facilitate parallel comparison with the FTIR data. (a) Comparison of FTIR and INS spectra over the region from 600–800 cm⁻¹. (b) INS spectra over the region from 375–450 cm⁻¹.

Table 1

NBO charges on each Zn atom in the phenoxy/Zn₁₂ model cluster depicted in Figure 2. Zn atoms bound to the phenoxy are indicated in bold. All charges are in units of the electron charge e .

atom	Charge without phenoxy (e)	Charge with phenoxy (e)	Difference (e)
1	0.676	0.656	-0.020
2	0.657	0.657	0.000
3	0.675	0.659	-0.016
4	0.676	0.652	-0.024
5	0.799	1.078	0.279
6	0.798	1.073	0.275
7	0.674	0.657	-0.017
8	0.657	0.651	-0.007
9	0.798	1.073	0.275
10	0.661	0.634	-0.027
11	0.675	0.660	-0.015
12	0.674	0.660	-0.013